coatings

MDPI

Article

Fabrication of a Flower-like Copper Oxide Film-Coated Nanoporous Stainless Steel Using Anodization-Assisted Electrodeposition as a Novel Antibacterial Material

Hefeng Wang [1,2,*], Naiming Lin [3], Jiaojiao Zhang [1], Yiwei Jia [1] and Hongting Zhao [1]

[1] College of Mechanical and Vehicle Engineering, Taiyuan University of Technology, Taiyuan 030024, China
[2] Institute of Applied Mechanics, Taiyuan University of Technology, Taiyuan 030024, China
[3] College of Materials Science and Engineering, Taiyuan University of Technology, Taiyuan 030024, China
* Correspondence: wanghefeng@tyut.edu.cn; Tel.: +86-0351-6010540

Abstract: In this study, flower-like copper oxide film was prepared on the surface of 316L nanoporous stainless steel (Cu/NPSS) by anodization-assisted electrodeposition. The prepared NPSS and Cu/NPSS were evaluated with Scanning electron microscopy (SEM), Energy dispersive X-ray spectroscopy (EDX) and X-ray diffractometer (XRD). Based on local use of common diseases, the antibacterial activity of Cu/NPSS against *Staphylococcus aureus* (*S. aureus*) and *Escherichia coli* (*E. coli*) was investigated. The diameters of the as-formed nanopores were about 93 nm at 50 V. Cu film was successfully deposited on the surface of NPSS. The presence of Cu and O was detected in the surface of Cu/NPSS by EDX analyses. The results obtained for Cu/NPSS revealed a marked antibacterial ability. The growth inhibition rates of Cu/NPSS against *E. coli* and *S. aureus* were 99.6% and 97.4% within 12 h, respectively. This may be because of the small size and high surface-to-volume ratio of the material in addition to the release of metal ions in solution. Accordingly, Cu/NPSS will help broaden promising applications in fields of biomedical implants and devices.

Keywords: nanoporous stainless steel; electrodeposition; anodization; copper; antibacterial activity

Citation: Wang, H.; Lin, N.; Zhang, J.; Jia, Y.; Zhao, H. Fabrication of a Flower-like Copper Oxide Film-Coated Nanoporous Stainless Steel Using Anodization-Assisted Electrodeposition as a Novel Antibacterial Material. *Coatings* **2023**, *13*, 782. https://doi.org/10.3390/coatings13040782

Academic Editor: Chi Tat Kwok

Received: 29 December 2022
Revised: 22 March 2023
Accepted: 23 March 2023
Published: 18 April 2023

1. Introduction

Stainless steel (SS), extensively used because of its outstanding corrosion resistance properties, does not possess anti-bacterial activity in biomedical applications [1,2]. Strong bacterial and viral adherence on SS surface may limit their long-term use in biological applications. If the antibacterial properties could be endowed on the surface of SS, it would broaden its application field.

Due to its adaptable porous structure and high active surface area, nanoporous materials have the capacity to adsorb and interact with atoms, ions, and molecules in the nanometer-sized pore space, which have the potential to be used in technology. As a result, the modification of the SS surface with nanostructure and the incorporation of oxide metals and noble metals has remarkable properties [3–5]. According to Rezaei, NPSS/Cu/Pd is a promising electrode for fuel cells and sensors' alcohol electrooxidation processes [6]. Zhan et al. prepared photocleanable stainless steel by anodization to form aligned nanopore arrays (NPAs) on the stainless steel surface [7]. Metal-based materials can be used in catalysis and can considerably increase the utilization of surface active sites and chemical reactions [8–10]. In order to avoid the first adherence of bacteria, there is, therefore, a great deal of interest in the design and manufacture of antibacterial agents (such as silver, copper, and zinc) on surfaces of nanoporous stainless steel (NPSS). We are aware of a limited amount of research that has addresses the use of antimicrobial NPSS as a substrate for biomedical devices such as artificial joints and dental implants.

Among these substances, copper and its oxides attracted the most interest because of their numerous benefits, including stability, cost effectiveness, and quick and efficient bacterial killing [11–13].

Highly ordered self-organized nanopores have been created on metal surfaces by electrochemical anodization on a large scale [14,15]. By using anodic oxidation and galvanic replacement process to adorn nanostructured gold within NPSS, Rezaei et al. demonstrated good repeatability and reproducibility, long-term stability, and adequate selectivity [14]. In order to assess the antibacterial activity and cytotoxicity of $Ti_{90-x}Cu_{10}Al_x$ (x = 0, 45) alloys produced by anodic oxidation of $Ti_{90-x}Cu_{10}Al_x$ in NH_4F-containing ethylene glycol electrolytes, Wang et al. used self-organized Cu-containing nano-tubes and $Ti_{90-x}Cu_{10}Al_x$ nanopores [15]. In addition, adding the right elements or metal oxides to well-ordered nanostructures can improve their electrochemical or antibacterial capabilities. A potentially effective bottom-up method for creating hard nanoporous templates is electrodeposition of metallic atoms into their nanopores. Simultaneously, incorporation of appropriate elements or metal oxides into well-ordered nanostructures can enhance antimicrobial activity or other electrochemical properties. An effective, low-cost bottom-up method for creating arrays of nanostructured materials is the electrodeposition of metallic atoms into the nanopores of hard nanoporous templates. For instance, Wu demonstrated that a straightforward and effective combined alternative current-direct current (AC-DC) electrodeposition method was successful in depositing Au nanowire arrays into an anodized aluminum oxide template [16]. Cobalt–nickel binary nanowires can be produced on nanoporous alumina membranes via AC electrodeposition, as demonstrated by Ali et al. [17]. Electrodeposition of Cu on NPSS (Cu/NPSS) has the potential to produce antimicrobial material.

The goal of this research was to investigate the antibacterial properties of Cu/NPSS made using anodization-assisted electrodeposition. These nanoporous materials display promising prospects due to their dual functionality, strong antibacterial activity, and nanoporous properties across a wide range of possible applications, including multifunctional coatings, healthcare-related environments, and biomedical devices and implants.

2. Experimental Methods

2.1. NPSS and Cu/NPSS Samples Preparation

The NPSS sample was prepared by anodization. Prior to anodization, SS electrode samples (Φ20 mm × 5 mm, Taiyuan Iron & Steel Group Co. LTD, Taiyuan, China) were polished with SiC papers (No. 400–1800). The sample was polished to mirror surface with diamond paste. Finally, the material was cleaned using ultrasonography in acetone and distilled water. SS sample served as the working electrode in a two-electrode electrochemical cell, while platinum foil gauge served as the counter electrode. As an electrolyte, ethylene glycol electrolyte with 5% $HClO_4$ was employed, and then anodized at a constant voltage of 20, 30, 40 and 50 V for 10 min. During anodization, the electrolyte temperature was kept at 0 °C. After anodization, the samples were washed in ethanol and distilled water and then dried under an air stream.

The Cu/NPSS sample was prepared by electrodeposition. The NPSS sample served as the working electrode during the electrodeposition process, while a saturated Ag/AgCl electrode served as the reference electrode, and a platinum sheet electrode served as the counter electrode on an electrochemical workstation (Gamry Reference 600). Deaerated solution of 0.1 M $Cu(CH_3COO)_2 \cdot H_2O$ and 0.1 M CH_3COONa was selected as electrolyte, and its pH value was adjusted to 5.7. The Cu/NPSS sample was prepared at a cathode potential of −1.0 V versus saturated Ag/AgCl for 3600 s. Figure 1 displays the prepared procedure of NPSS and Cu/NPSS sample.

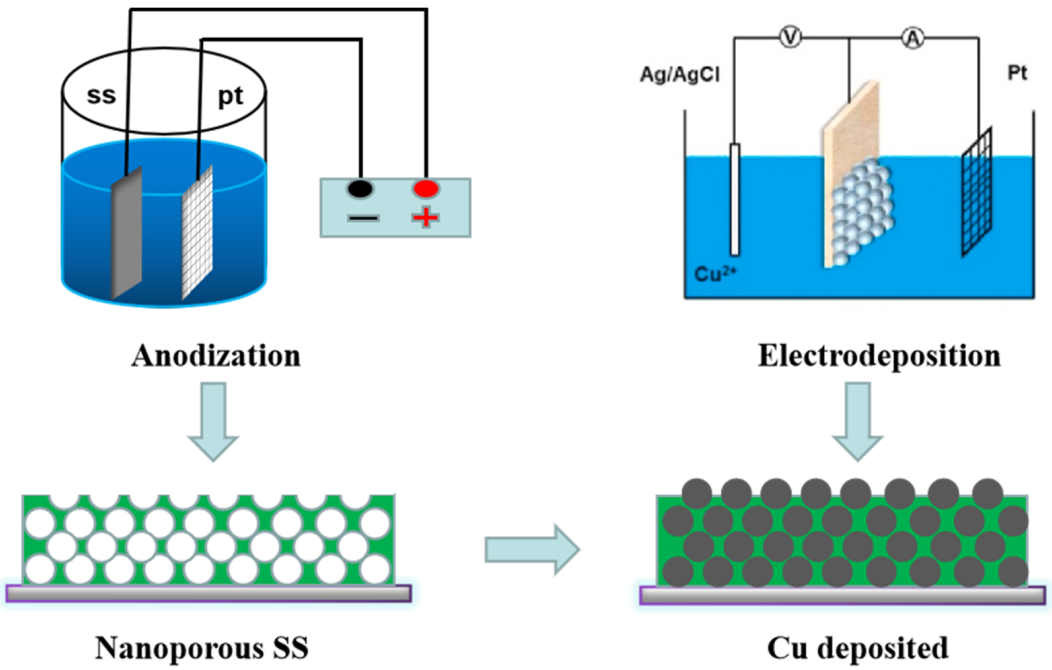

Figure 1. Procedure diagram for preparing NPSS and Cu/NPSS.

2.2. Sample Characterization

By using a Cu target (=1.5410) as the excitation source, an X-ray diffractometer (D/max-2550-18 kW, Rigaku, Japan) was used to study the crystal structures of NPSS and Cu/NPSS. NPSS and Cu/NPSS were examined for morphology and composition using a field-emission scanning electron microscope (JSM-7001F, JEOL, Tokyo, Japan) that was equipped with an energy-dispersive X-ray source (EDX, JSM-7001F, JEOL, Tokyo, Japan).

2.3. In Vitro Bactericidal Activity

By using spread plate counts, the antibacterial activity of the samples (NPSS and Cu/NPSS samples) was assessed. This study made use of the bacteria *Staphylococcus aureus* (*S. aureus*) and *Escherichia coli* (*E. coli*). The testing samples were put in Petri dishes that had been sterilized. Then, 0.4 mL of a bacterial solution that contained 10^5 CFU/mL was dripped on the surface of samples. The dishes were then incubated for 12 h at 37 °C with a humidity of 90%. After incubation, 0.9 mL of phosphate buffer solution washing was used to collect the bacteria into a sterile Petri dish. The active bacteria were then counted after 0.1 mL of the aforementioned washing solution was put on a nutrient agar plate and incubated at 37 °C for 24 h.

The antibacterial rate R was calculated by the following formula:

$$R = \left[\frac{\lambda_0 - \lambda_t}{\lambda_0}\right] \times 100\% \quad (1)$$

where λ_t and λ_0 are the average numbers of viable bacterial colony on the sample, respectively.

3. Results and Discussions

3.1. Composition and Phase Characterization of NPSS and Cu/NPSS Samples

The XRD spectra of NPSS and Cu/NPSS are illustrated in Figure 2. The crystal structure of NPSS exhibited the major diffraction peaks at ca. 44° and 51°, which corresponded to austenite phase. The Cu/NPSS crystal structure is mostly composed of the austenite phase, which contains CuO, and Cu_2O. Here, the Cu_2O phase that was obtained agrees with previous report [18].

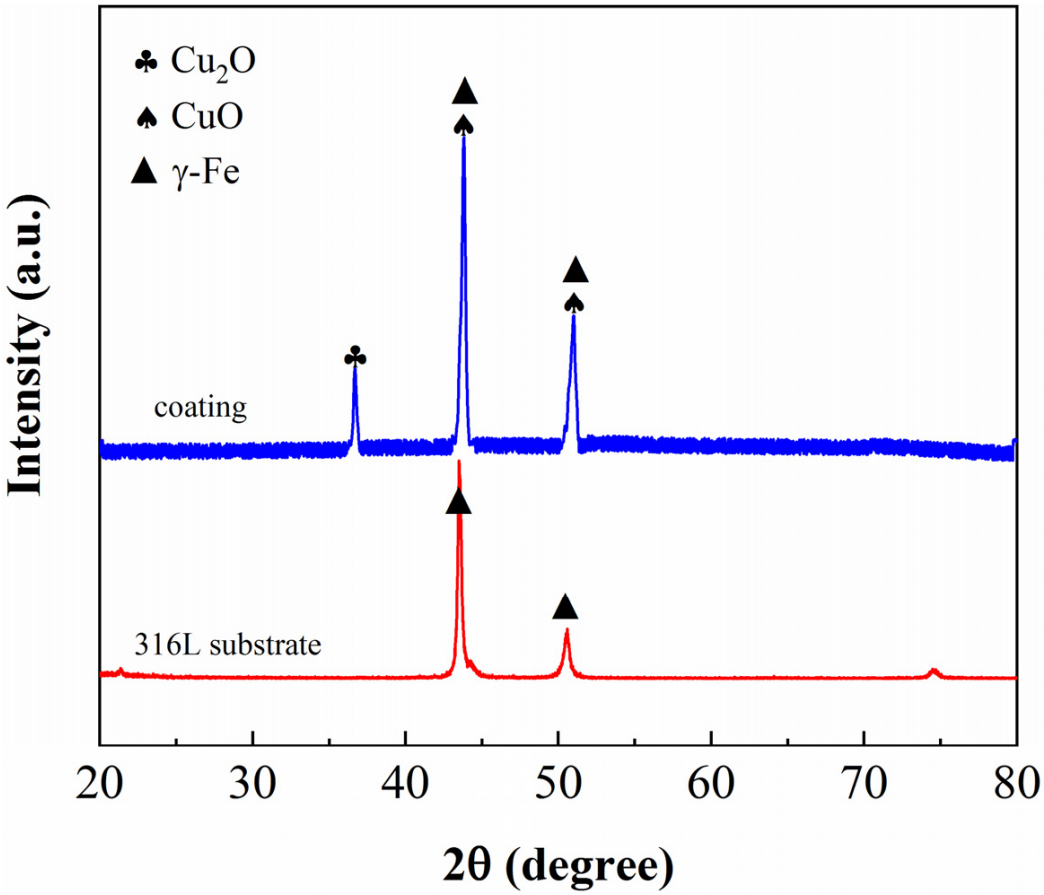

Figure 2. XRD spectra of the NPSS and Cu/NPSS samples.

3.2. Microstructural of NPSS and Cu/NPSS Samples

As revealed in Figure 3, nanopore structure can be formed on the surface of 316L SS at different anodizing voltages. The surface exhibited a quasi-periodic arrangement of pores, which can be obtained at voltages of 40 and 50 V (as shown in Figure 3b,c). The findings demonstrate that the nanopore structure at 50 V, which has an estimated value of 93 nm and 87 nm, is slightly larger than that at 40 V. Subsequently, SS samples after anodizing at 50 V were used as research objects.

SEM and EDX were used to analyze the surface morphology of the Cu/NPSS (Figure 4). The surface of NPSS was covered in dendritic crystals. These morphologies do indeed resemble those that have already been reported [19–21]. The typical copper dendritic formations' mechanism was explained using the diffusion-limited aggregation (DLA) hypothesis. This is thus because copper deposits that resemble DLA are frequently found in polycrystalline copper branches. This result indicates that the nanopore structure SS significantly improves the electrodeposition of dendrite copper films due to versatile porous structure and high active surface area. Such a flower-like Cu film-coated nanoporous stainless steel has an excellent membrane base binding strength. This is due to the fact that nanopore structures improve the capacity for atom absorption and interaction. It was clear from the EDX and XRD data of Cu/NPSS in Figures 2 and 4 that an electrodeposited copper oxide coating had formed on the surface of 316L NPSS.

3.3. Antimicrobial Activities of NPSS and Cu/NPSS Samples

As seen from Figure 5, NPSS does not display antibacterial activity. According to Figure 5a, the *E. coli* bacterial colonies from the NPSS surface are virtually evenly distributed around the Petri dish, showing that the NPSS has little antimicrobial effect against *E. coli*. However, it was determined that the Cu/NPSS sample's live *E. coli* colonies were all but

gone (Figure 5b). Similar to the NPSS surface, the Cu/NPSS surface can also acquire a significant antibacterial action for the growth suppression of Gram-positive *S. aureus* colonies (Figure 6a). Only a small number of viable *S. aureus* colonies could be seen in the Cu/NPSS sample, as shown in Figure 6b. Cu/NPSS had typical bactericidal efficiencies of 99.6% and 97.4 against *E. coli* and *S. aureus*, respectively (see Table 1).

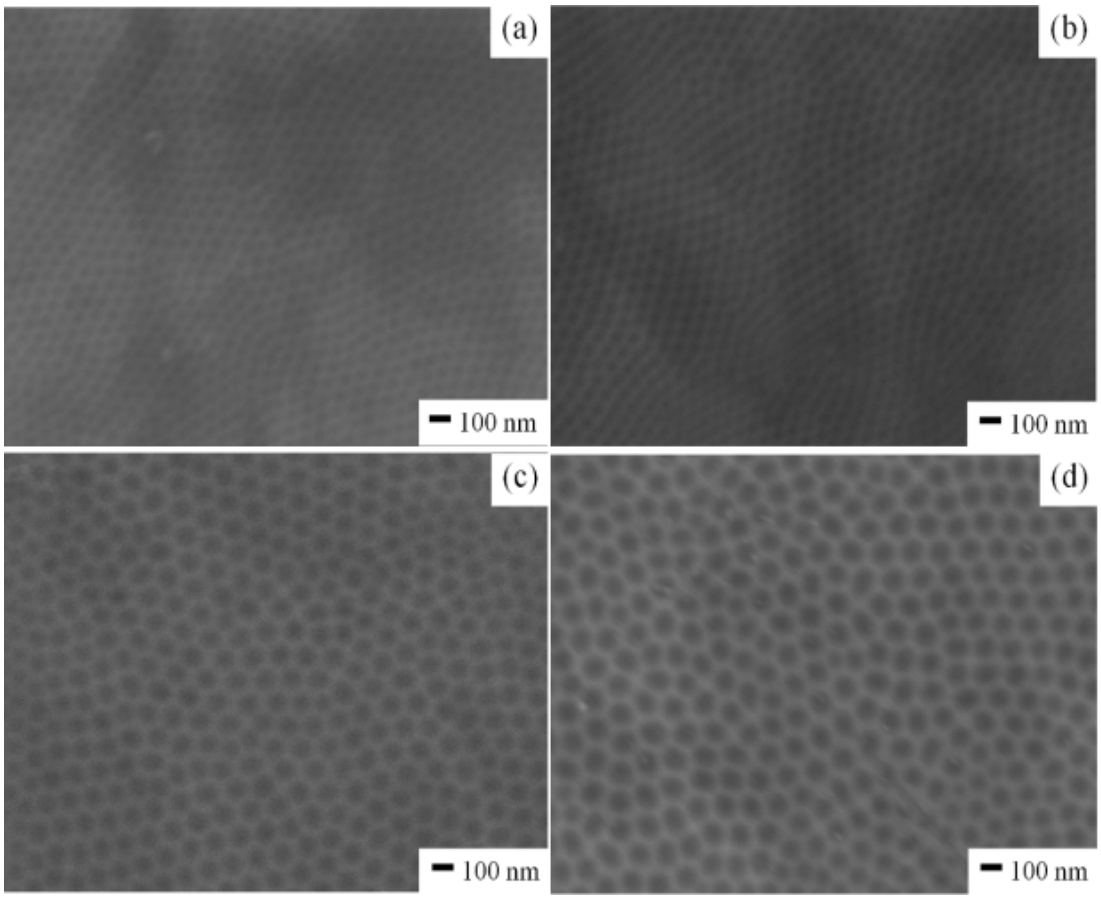

Figure 3. Morphologies of anodic oxidation stainless steel electrode in the ethylene glycol electrolyte containing $HClO_4$ at potentials of 20 (**a**), 30 (**b**), 40 (**b**) and 50 V (**d**).

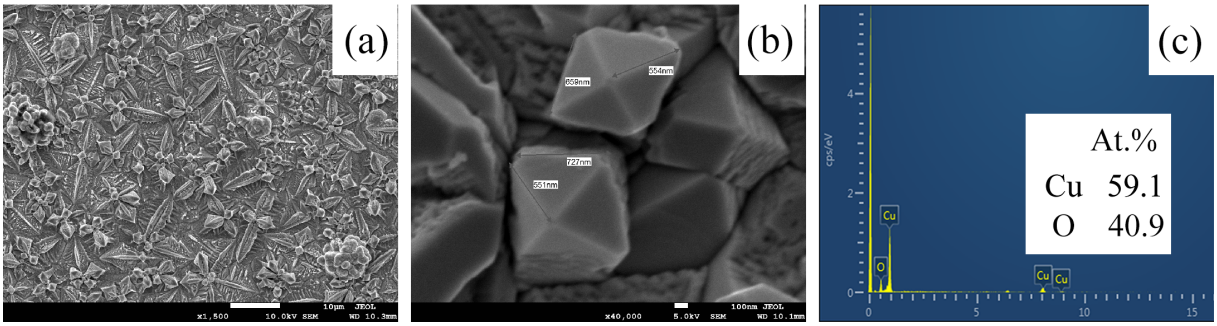

Figure 4. SEM image of Cu/NPSS (**a**), magnification image of the Cu/NPSS (**b**) and the corresponding atomic ratios of elements of the Cu/NPSS (**c**).

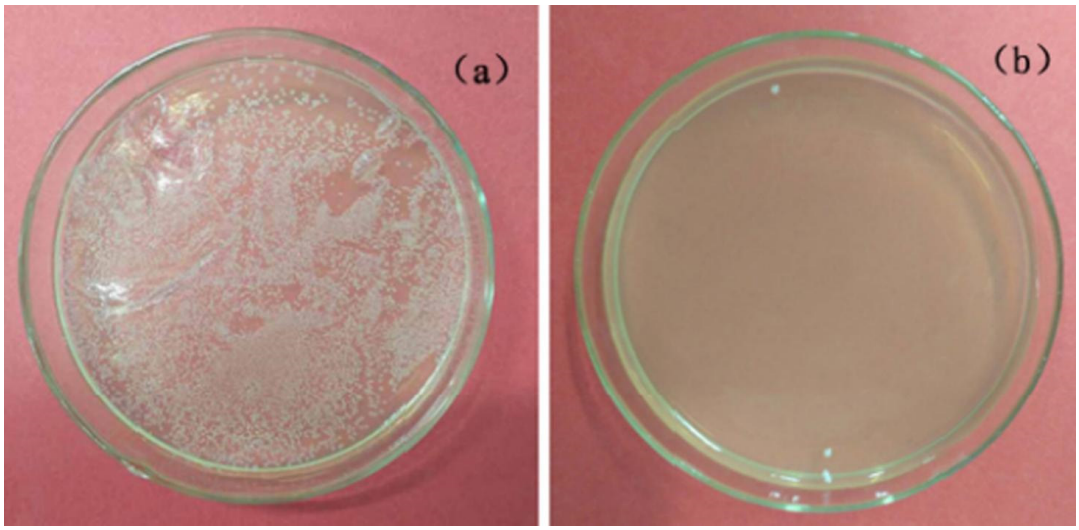

Figure 5. *E. coli* bacterial colonies on different samples after a 12 h incubation. (**a**) NPSS, (**b**) Cu/NPSS.

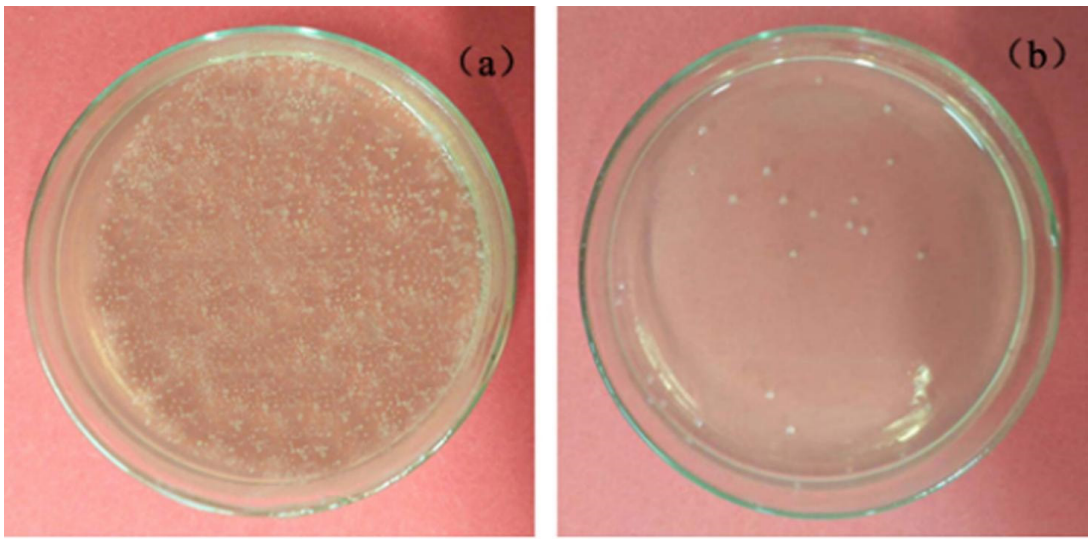

Figure 6. *S. aureus* bacterial colonies on different samples after a 12 h incubation. (**a**) NPSS, (**b**) Cu/NPSS.

Table 1. The bacterial test results for the Cu/NPSS sample.

Strain	Bacterial Reduction Rate
E. coli	99.6%
S. Aureus	97.4%

It has been agreed that membrane destruction is the primary effect of sterilization on bacterial cells [22,23]. Several studies have shown that copper and silver ions attach to cell walls of negatively charged bacteria, damaging the permeability of cell walls. This effect is associated with protein-induced cell lysis and death [24]. According to Li et al., dissolved copper ions play a leading role in antimicrobial action, resulting in the collapse of some lipid polysaccharide patches on the surface of the cell, which alters the permeability and functionality of the outer cell membrane [25]. Zhang et al. also reported that cell walls and membranes dissolve when they come in contact with surfaces that contain copper, which causes inner cytoplasm to flow out [11]. Wang et al. reported that the sterilization effect of TiCu-O and TiAlCu-O layers is caused by the release of Cu^{2+} due to contact with

the bacterial solution [15]. Zhang et al. indicated that the bacteria are killed in contact with Ti_2Cu antibacterial phase, and that fine high surface area Ti_2Cu phases show high antibacterial ability [26]. Several solid-state cuprous compounds, such as cuprous oxide (Cu_2O), sulfide (Cu_2S), iodide (CuI), and chloride (CuCl), have been reported to have highly effective antiviral properties. Kayano Sunada et al. also discovered that Cu_2O adsorbed and denatured more proteins than CuO [27]. As a result of the presence of antiviral agents, such as metal atoms, synthetic or natural polymers, and tiny molecules, according to Ostap Lishchynskyic et al., viruses can become biologically inert upon interaction with active antiviral surfaces [28].

According to this study, the bacteria may be effectively killed by the CuO and Cu_2O implanted within the nanoporous layer. The release of Cu^{2+} when the surface comes in contact with the bacterial solution is what causes the bactericidal action of these in situ Cu-doped nanoporous layers.

It has been widely reported that porous metal bone implant material shows great potential for bone regeneration [29,30]. Herein, in situ Cu-doped nanoporous layers by anodizatio-electrodeposition not only exhibit almost equal antibacterial activity, but also provide a more favorable bioactive environment for osteoblast cell proliferation. Seunghan et al. indicated that osteoblast cells adhesion/propagation on the morphology of the nanotubes obviously improved, and the developing cells' filopodia actually entered the holes of the nanotubes to form an interlocking cell structure [30].

In any case, this hybrid kind of self-organized Cu-containing nanoporous layer with excellent antimicrobial ability will find potential applications in areas such as antimicrobial materials, biomedicine or implants.

4. Conclusions

In conclusion, anodization-assisted electrodeposition was successful in creating a flower-like copper oxides film on NPSS. The Cu/NPSS is mainly composed of Cu_2O and CuO phases, as well as an appropriate nanoporous structure with a mean diameter of 93 nm at 50 V. The results obtained for Cu/NPSS revealed a marked antibacterial ability. The growth inhibition rates of Cu/NPSS against *E. coli* and *S. aureus* were 99.6% and 97.4% within 12 h, respectively. This may be because of the small size of the small size and high surface-to-volume ratio of the material in addition to the release of metal ions in solution. Accordingly, Cu/NPSS will help broaden promising applications in the area of biological implants and devices.

Author Contributions: Conceptualization, H.W. and N.L.; methodology, H.W.; validation, H.W., N.L. and J.Z.; investigation, J.Z., Y.J. and H.Z.; writing—review and editing, H.W.; project administration, H.W. and N.L. All authors have read and agreed to the published version of the manuscript.

Funding: The authors are grateful to the National Natural Science Foundation of China (11772217). Research Project of Returned Overseas Students in Shanxi Province (2020-030). Preference Funding Project for Science and Technology Activities of Overseas Students in Shanxi Province (20200028). China-belarus Joint Laboratory for the Belt and Road Initiative (ZBKF2022031101).

Institutional Review Board Statement: Not applicable.

Informed Consent Statement: Not applicable.

Data Availability Statement: Not applicable.

Conflicts of Interest: The authors declare no conflict of interest.

References

1. Muthupandi, V.; Srinivasan, P.B.; Seshadri, S.; Sundaresan, S. Effect of weld metal chemistry and heat input on the structure and properties of duplex stainless steel welds. *Mater. Sci. Eng. A* **2003**, *358*, 9–16. [CrossRef]
2. Hong, I.T.; Koo, C.H. Antibacterial properties, corrosion resistance and mechanical properties of Cu-modified SUS 304 stainless steel. *Mater. Sci. Eng. A* **2005**, *393*, 213–222. [CrossRef]
3. Liu, Z.; Liu, B.; Ding, D.; Jiang, Z.; Xia, C. Development of three-layer intermediate temperature solid oxide fuel cells with direct stainless steel based anodes. *Int. J. Hydrogen Energy* **2012**, *37*, 4401–4405. [CrossRef]
4. Wyrwa, D.W.; Schmid, G. Metal Nanoparticles on Stainless Steel Surfaces as Novel Heterogeneous Catalysts. *J. Clust. Sci.* **2007**, *18*, 476–493. [CrossRef]
5. Wu, H.-B.; Niu, G.; Wu, F.-J.; Tang, D. Reverse-transformation austenite structure control with micro/nanometer size. *Int. J. Miner. Met. Mater.* **2017**, *24*, 530–537. [CrossRef]
6. Rezaei, B.; Havakeshian, E.; Ensafi, A.A. Fabrication of a porous Pd film on nanoporous stainless steel using galvanic replacement as a novel electrocatalyst/electrode design for glycerol oxidation. *Electrochim. Acta* **2014**, *136*, 89–96. [CrossRef]
7. Zhan, W.; Ni, H.; Chen, R.; Song, X.; Huo, K.; Fu, J. Formation of nanopore arrays on stainless steel surface by anodization for visible-light photocatalytic degradation of organic pollutants. *J. Mater. Res.* **2012**, *27*, 2417–2424. [CrossRef]
8. Roy, P.; Berger, S.; Schmuki, P. TiO_2 Nanotubes: Synthesis and Applications. *Angew. Chem. Int. Ed.* **2011**, *50*, 2904–2939. [CrossRef]
9. Nah, Y.-C.; Paramasivam, I.; Schmuki, P. Doped TiO_2 and TiO_2 Nanotubes: Synthesis and Applications. *Chem. Phys. Chem.* **2010**, *11*, 2698–2713. [CrossRef]
10. Liang, Y.Q.; Cui, Z.D.; Zhu, S.L.; Liu, Y.; Yang, X.J. Silver nanoparticles supported on TiO_2 nanotubes as active catalysts for ethanol oxidation. *J. Catal.* **2011**, *278*, 276–287. [CrossRef]
11. Zhang, X.; Ma, Y.; Lin, N.; Huang, X.; Hang, R.; Fan, A.; Tang, B. Microstructure, antibacterial properties and wear resistance of plasma Cu–Ni surface modified titanium. *Surf. Coat. Technol.* **2013**, *232*, 515–520. [CrossRef]
12. Akhavan, O.; Ghaderi, E. Cu and CuO nanoparticles immobilized by silica thin films as antibacterial materials and photocatalysts. *Surf. Coat. Technol.* **2010**, *205*, 219–223. [CrossRef]
13. Chan, Y.H.; Huang, C.F.; Ou, K.L.; Peng, P.W. Mechanical properties and antibacterial activity of copper doped diamond-like carbon films. *Surf. Coat. Technol.* **2011**, *206*, 1037–1040. [CrossRef]
14. Rezaei, B.; Havakeshian, E.; Ensafi, A.A. Decoration of nanoporous stainless steel with nanostructured gold via galvanic replacement reaction and its application for electrochemical determination of dopamine. *Sens. Actuators B* **2015**, *213*, 484–492. [CrossRef]
15. Wang, X.; Qiao, J.; Yuan, F.; Hang, R.; Huang, X.; Tang, B. In situ growth of self-organized Cu-containing nano-tubes and nano-pores on Ti90−xCu10Alx (x = 0, 45) alloys by one-pot anodization and evaluation of their antimicrobial activity and cytotoxicity. *Surf. Coat. Technol.* **2014**, *240*, 167–178. [CrossRef]
16. Wu, Z.; Zhang, Y.; Du, K. A simple and efficient combined AC–DC electrodeposition method for fabrication of highly ordered Au nanowires in AAO template. *Appl. Surf. Sci.* **2013**, *265*, 149–156. [CrossRef]
17. Ali, G.; Maqbool, M. Fabrication of cobalt-nickel binary nanowires in a highly ordered alumina template via AC electrodeposition. *Nanoscale Res. Lett.* **2013**, *8*, 1–8. [CrossRef]
18. Zhu, S.L.; He, J.L.; Yang, X.J.; Cui, Z.D.; Pi, L.L. Ti oxide nano-porous surface structure prepared by dealloying of Ti-Cu amorphous alloy. *Electrochem. Commun.* **2011**, *13*, 250–253. [CrossRef]
19. Nikolić, N.D.; Popov, K.I.; Pavlović, L.J.; Pavlović, M.G. Morphologies of copper deposits obtained by the electrodeposition at high overpotentials. *Surf. Coat. Technol.* **2006**, *201*, 560–566. [CrossRef]
20. Popov, K.I.; Nikolic, N.D.; Rakočević, Z.L. An estimation of the interfacial energy of the copper–copper sulphate solution interface and of the specific surface of cop- per powder. *J. Serb. Chem. Soc.* **2002**, *67*, 635–638. [CrossRef]
21. Popov, K.I.; Nikolic, N.D.; Rakočević, Z.L. The estimation of solid copper surface tension in copper sulfate solutions. *J. Serb. Chem. Soc.* **2002**, *67*, 769–775. [CrossRef]
22. Santo, C.E.; Lam, E.W.; Elowsky, C.G.; Quaranta, D.; Domaille, D.W.; Chang, C.J.; Grass, G. Bacterial Killing by Dry Metallic Copper Surfaces. *Appl. Environ. Microbiol.* **2011**, *77*, 794–802. [CrossRef] [PubMed]
23. Ibrahim, M.; Wang, F.; Lou, M.-M.; Xie, G.-L.; Li, B.; Bo, Z.; Zhang, G.-Q.; Liu, H.; Wareth, A. Copper as an antibacterial agent for human pathogenic multidrug resistant Burkholderia cepacia complex bacteria. *J. Biosci. Bioeng.* **2011**, *112*, 570–576. [CrossRef] [PubMed]
24. Lin, Y.E.; Vidic, R.D.; Stout, J.E.; Mccartney, C.A.; Yu, V.L. Inactivation of mycobacterium avium by copper and silver ions. *Water Res.* **1998**, *32*, 1997–2000. [CrossRef]
25. Nan, L.; Liu, Y.; Lü, M.; Yang, K. Study on antibacterial mechanism of copper–bearing austenitic antibacterial stainless steel by atomic force microscopy. *J. Mater. Sci. Mater. Med.* **2008**, *19*, 3057–3062. [CrossRef] [PubMed]
26. Zhang, E.; Li, F.; Wang, H.; Liu, J.; Wang, C.; Li, M.; Yang, K. A new antibacterial titanium–copper sintered alloy: Preparation and antibacterial property. *Mater. Sci. Eng. C* **2013**, *33*, 4280–4287. [CrossRef]
27. Lishchynskyi, O.; Shymborska, Y.; Stetsyshyn, Y.; Raczkowska, J.; Skirtach, A.G.; Peretiatko, T.; Budkowski, A. Passive antifouling and active self-disinfecting antiviral surfaces. *Chem. Eng. J.* **2022**, *446*, 137048. [CrossRef]
28. Sunada, K.; Minoshima, M.; Hashimoto, K. Highly efficient antiviral and antibacterial activities of solid-state cuprous compounds. *J. Hazard. Mater.* **2012**, *235–236*, 265–270. [CrossRef]

29. Wen, C.E.; Mabuchi, M.; Yamada, Y.; Shimojima, K.; Chino, Y.; Asahina, T. Processing of biocompatible porous Ti and Mg. *Scr. Mater.* **2001**, *45*, 1147–1153. [CrossRef]
30. Oh, S.; Daraio, C.; Chen, L.H.; Pisanic, T.R.; Fiñones, R.R.; Jin, S. Significantly accelerated osteoblast cell growth on aligned TiO_2 nanotubes. *J. Biomed. Mater. Res.* **2006**, *78*, 97–103. [CrossRef]